Angiogenesis (2019) 22:281–293
https://doi.org/10.1007/s10456-018-9656-z

ORIGINAL PAPER

TSPYL5-mediated inhibition of p53 promotes human endothelial cell function

Hee-Jun Na[1] · Chung Eun Yeum[1] · Han-Seop Kim[1] · Jungwoon Lee[1] · Jae Yun Kim[1,2] · Yee Sook Cho[1,2]

Received: 14 August 2018 / Accepted: 20 November 2018 / Published online: 23 November 2018

Abstract

Testis-specific protein, Y-encoded like (TSPYL) family proteins (TSPYL1-6), which are members of the nucleosome assembly protein superfamily, have been determined to be involved in the regulation of various cellular functions. However, the potential role of TSPYL family proteins in endothelial cells (ECs) has not been determined. Here, we demonstrated that the expression of TSPYL5 is highly enriched in human ECs such as human umbilical vein endothelial cells (HUVECs) and human pluripotent stem cell-differentiated ECs (hPSC-ECs). Importantly, TSPYL5 overexpression was shown to promote EC proliferation and functions, such as migration and tube formation, by downregulating p53 expression. Adriamycin-induced senescence was markedly blocked by TSPYL5 overexpression. In addition, the TSPYL5 depletion-mediated loss of EC functions was blocked by p53 inhibition. Significantly, TSPYL5 overexpression promoted angiogenesis in Matrigel plug and wound repair in a mouse skin wound healing model in vivo. Our results suggest that TSPYL5, a novel angiogenic regulator, plays a key role in maintaining endothelial integrity and function. These findings extend the understanding of TSPYL5-dependent mechanisms underlying the regulation of p53-related functions in ECs.

Keywords TSPYL5 · Endothelial cells · Proliferation · Angiogenesis · p53

Introduction

Y chromosome-located TSPY (testis-specific protein, Y-encoded), which is a member of the nucleosome assembly protein (NAP) family, harbors a conserved SET (suppressor of variegation, enhancer of zeste and Trithorax)/NAP domain [1, 2] and is abundantly expressed and functional in normal germ cells of fetal and adult testes and various testicular tumors [1–5]. TSPY-like (TSPYL) genes sharing significant homology with TSPY (including *TSPYL1–TSPYL6*) have been identified on the non-sex chromosomes (autosomes) or the X chromosome [6, 7], unlike TSPY itself, which exerts male-specific effects. TSPY-like genes are ubiquitously and heterogeneously expressed in various human tissues [6, 8].

Functional roles of TSPYL family members involved in a wide spectrum of biological processes have been demonstrated in various tissue and cell types. TSPYL2 [also known as calmodulin-associated serine/threonine kinase (CASK)-interacting NAP, CINAP] is highly expressed in the brain [9, 10]. The interaction of TSPYL2 with calcium/calmodulin-dependent serine protein kinase (CASK), an X-linked member of the membrane-associated guanylate kinase (MAGUK) family of proteins and T-box brain gene 1 (Tbr-1), is important for neural development and function [11, 12]. The TSPYL2/REST complex (a transcriptional repressor of neuronal genes) acts as a tumor repressor by promoting TGFβ signaling through suppressing the expression of TGFβ target genes such as neurotrophic tyrosine kinase receptor C (TrkC) in human mammary epithelial cells [13].

Hee-Jun Na, Chung Eun Yeum and Han-Seop Kim have contributed equally to this work.

Electronic supplementary material The online version of this article (https://doi.org/10.1007/s10456-018-9656-z) contains supplementary material, which is available to authorized users.

✉ Yee Sook Cho
june@kribb.re.kr

[1] Stem Cell Research Laboratory, Immunotherapy Convergence Research Center, Korea Research Institute of Bioscience and Biotechnology, 125 Gwahak-ro, Yuseong-gu, Taejon 34141, Republic of Korea

[2] Department of Bioscience, KRIBB School, University of Science & Technology, 113 Gwahak-ro, Yuseong-gu, Taejon 34113, Republic of Korea

Aberrant expression and/or dysregulation of TSPYL family proteins is associated with a variety of diseases, including tumors [14, 15]. The mutated *TSPYL1* gene, encoding a protein with a deleted TSPY/NAP/SET domain, is responsible for sudden infant death with dysgenesis of the testes syndrome (SIDDT) [16]. Altered expression of the *TSPYL1* gene has also been implicated in the high levels of γ-globin observed in deletional hereditary persistence of fetal hemoglobin and δβ-thalassemia [17]. Duplication of the TSPYL2 gene at Xp11.2 is strongly suspected to cause intellectual disability, possibly by disturbing synaptic signaling [18]. TSPYL was found to be involved in the recruitment of nucleoplasmic zinc finger protein 106 (ZFP106) into nuclear bodies, and loss of proper nuclear targeting of ZFP106 is potentially responsible for TSPYL-associated diseases, such as SIDDT [19]. TSPYL5, known as a marker of poor prognosis in breast cancer, was shown to be responsible for the increased biosynthesis of E2 and increased levels of circulating E1 in postmenopausal women with estrogen receptor (ER)-positive breast cancer [20].

The ubiquitous expression of TSPYL family proteins implies their varying roles in diverse tissues and cell types; however, their exact roles in EC-specific expression and functions are not yet understood. The present study was performed to determine and characterize endothelial cell-specific functional roles of TSPYL family proteins and the probable mechanism(s) underlying TSPYL-mediated EC regulation, with an aim of exploring the potential link between TSPYL and angiogenesis. Our results uncover an essential role for TSPYL5 as a positive regulator of human EC functions, including EC-mediated angiogenesis, and we further demonstrate that TSPYL-promoted EC functions is mediated by p53 inhibition.

Materials and methods

Antibodies

The following antibodies were used in this study: TSPYL5, USP7, and β−αχτιν (Αβχαμ, Χαμβριδγε, MA, ΥΣΑ); π53, $\pi 21^{WAF1/CIP1}$, and β−tubulin (Santa Cruz Biotechnology, CA, USA); and Sirt1 and horseradish peroxidase (HRP)-conjugated secondary antibodies (Thermo Fisher Scientific, Waltham, MA, USA).

Reagents

Pifithrin-α (PFT-α) was purchased from Biomol (Enzo Life Sciences Inc., PA, USA). A stock solution of PFT-α (1 mM) was prepared in dimethyl sulfoxide (≥ 99.9%, Sigma-Aldrich, San Louis, MO, USA). Adriamycin (Doxorubicin) was purchased from Sigma (St. Louis, MO). A stock solution of adriamycin (1.8 mM) was prepared in phosphate-buffered saline (PBS). Vascular endothelial growth factor (VEGF) and basic fibroblast growth factor (bFGF) were purchased from Upstate Biotechnology (Lake Placid, NY, USA). Cell culture reagents were purchased from Invitrogen Life Technologies (Carlsbad, CA, USA) unless otherwise indicated. The hematoxylin and eosin (H&E) staining kit was purchased from Thermo Fisher Scientific (San Jose, CA, USA), and Masson's Trichrome Staining Kit was purchased from Sigma (St. Louis, MO).

Cell culture

Human umbilical vein endothelial cells (HUVECs) were purchased from Lonza (Walkersville, MD, USA) and cultured in Medium 199 (Invitrogen Corporation, Carlsbad, CA, USA) containing 20% fetal bovine serum, 100 units/ml penicillin, 100 ng/ml streptomycin, 3 ng/ml bFGF, and 5 units/ml heparin at 37 °C under 5% CO_2/95% air. H9 human ESCs (WA09 lines, WiCell Research Institute, Inc., Madison, WI) and normal human iPSCs [21] were maintained under a feeder-free condition in mTeSR1 (ST05850; StemCell Technology, Vancouver, British Columbia, Canada) on Matrigel-coated tissue culture dishes at 37 °C under 5% CO_2/95% air. For embryoid body (EB) formation, dissociated hESCs or hiPSCs with 1 mg/ml collagenase IV were transferred to non-cell culture-treated Petri dishes and cultured in EB culture medium consisting of KnockOut DMEM supplemented with 10% KSR, 1% NEAA, 0.1 mM β-mercaptoethanol and 1 mM L-glutamine. 7-day-old EBs were used for further analysis.

Semiquantitative reverse-transcriptase polymerase chain reaction (RT-PCR) and quantitative real-time PCR (qPCR)

For the PCR analysis, total RNA was extracted from cells with an RNeasy Mini Kit (Qiagen, Hilden, Germany) and reverse transcribed with a SuperScript First-strand Synthesis System Kit (Invitrogen) according to the manufacturer's instructions. Semiquantitative RT-PCR was performed using a platinum Tag Super Mix kit (Invitrogen). The reaction conditions were as follows: pre-denaturation at 94 °C for 3 min, followed by 30 cycles of denaturation at 94 °C for 30 s, annealing at 60 °C for 30 s, and elongation at 72 °C for 20 s.

QPCR was performed with the QuantiTect SYBR Green PCR Master Mix (Qiagen) on an ABI PRISM 7500 Real-Time PCR System (Applied Biosystems, Carlsbad, CA). The reaction conditions were as follows: pre-denaturation at 94 °C for 10 min, followed by 40 cycles of denaturation at 94 °C for 15 s, annealing at 60 °C for 1 min, and elongation at 72 °C for 30 s. Each experiment was performed at least three times. The relative fold changes in target gene

expression were calculated using the comparative $2^{-\Delta\Delta Ct}$ method, and the GAPDH gene was used to normalize the cDNA concentration of each gene. The primer sequences are summarized in Supporting Table 1.

Overexpression or knockdown of TSPYL5

For the overexpression experiments, the TSPYL5 expression vector construct (pMX-TSPYL5) was generated by inserting the entire TSPYL5 coding region (GenBank accession number: BC045630) into the pMXs (pMXs-IP:IRES-puro; pMX-puro) retrovirus system (Addgene, Cambridge, MA, USA). Cells were transfected with a pMX retroviral supernatant supplemented with 4 μg/ml polybrene (Millipore). For the selection of stably transfected cells 2 days posttransfection, cells were incubated with selective culture media containing 10 μg/ml puromycin (Sigma), and freshly prepared selective media was replaced every 2–3 days thereafter. Cells were also transfected with the control, pMXs-GFP (pMXs-IG:IRES-GFP, Addgene). TSPYL5 overexpression was assessed by measuring the levels of TSPYL5 mRNA and protein using real-time PCR and Western blotting, respectively.

For the knockdown of TSPYL5 expression, cells were transfected with TSPYL5 shRNA lentiviral particles (Lenti-shTSPYL) generated from TSPYL5 shRNA plasmid (Cat# sc-77735-SH, Santa Cruz Biotechnology, Inc., CA, USA) in 293FT cells according to the manufacturer's instructions. Cells were also transfected with control shRNA (sc-108060, Santa Cruz Biotechnology, Inc.). For the selection of stably transfected cells 2 days posttransfection, cells were incubated with selective culture media containing 5 μg/ml puromycin, and freshly prepared selective media was replaced every 2–3 days thereafter. The knockdown of TSPYL5 expression was assessed by measuring the levels of TSPYL5 mRNA and protein using real-time PCR and Western blotting, respectively.

Cell proliferation assays

Cell proliferation was determined with CCK-8 assays (Dojindo, Japan) according to manufacturer's instructions. Cells were seeded onto 96-well plates at 2×10^3 cells/well. After attachment, cells were transfected with the control (empty vector or no treatment), pMX-TSPYL5, or lenti-shTSPYL5 in the presence or absence of PFT-α and incubated in culture medium at 37 °C and 5% CO_2. The CCK-8 solution was added to each well at the indicated times, and the plates were incubated for an additional 2 h at 37 °C and 5% CO_2. Cell viability was calculated based upon the OD value at 450 nm obtained with a microplate reader (BioTek Synergy HT) according to the manufacturer's instructions. Average values from at least three independent experiments were used to analyze the data.

Endothelial cell migration assay

The chemotactic motility of ECs was assessed using Transwell plates with 6.5-mM diameter polycarbonate filters (Corning-Costar Corp., Cambridge, MA, USA). The lower surface of the filter was coated with 10 μg of gelatin. ECs transfected with the control (empty vector or no treatment), pMX-TSPYL5, or lenti-shTSPYL5 in the presence or absence of PFT-α were trypsinized and suspended at a final concentration of 1×10^6 cells/ml in Medium 199. Fresh EGM-2 medium was placed in the lower wells, and 100 μl of the cell suspension was loaded into the upper wells. The chamber was incubated at 37 °C for 4 h, and then, the cells were fixed and stained with H&E in the standard fashion. Non-migrating cells on the upper surface of the filter were removed by wiping with a cotton swab, and chemotaxis was quantified by counting the cells that had migrated to the lower side of the filter at low-power magnification (×100) by using an inverted microscope.

Tube formation assay

Vascular tube-like formation by endothelial cells on growth factor-reduced Matrigel was assayed as previously described [22]. Briefly, 12-well culture plates were coated with 250 μl of Matrigel, which was allowed to polymerize for 30 min at 37 °C. Endothelial cells cultured in EGM-2 medium for 6 h were plated onto the layer of Matrigel at a density of 4×10^5 cells/well. Matrigel cultures were incubated at 37 °C for 20 h. Tube formation was observed using an inverted phase contrast microscope and images were captured by a video graphic system.

Senescence assay

For the cytochemical assessment of β-galactosidase positive cells, cells were plated in 6-well culture dishes at a density of 5×10^4 cells/cm^2. After 1 day, cells were transfected with either an empty vector or a TSPYL5 overexpression vector in the presence or absence of adriamycin and then incubated for 2 days. Senescence-associated β-galactosidase (SA-β-gal) activity was detected with the Cellular Senescence Assay kit (EMD Millipore, USA).

Western blot analysis

Protein lysates were prepared in RIPA buffer (50 mmol/l Tris–HCl, pH 8.0, 150 mM sodium chloride, 1% Triton X-100, 0.5% deoxycholic acid, and 0.1% SDS), and protein concentration was determined by the bicinchoninic

acid (BCA) assay using bovine serum albumin (BSA) as the standard. Protein lysates (60 μg of protein) were separated by SDS-PAGE (sodium dodecyl sulfate-polyacrylamide gel electrophoresis) and transferred onto a polyvinylidene difluoride membrane. After blocking in 5% BSA in Tris-buffered saline/0.05% Tween 20 (TBS-T) for 30 min, the membranes were incubated with the indicated primary antibodies (TSPYL5, USP7, p53, p21, Sirt1, and β-actin) overnight, washed, and incubated with horseradish peroxidase-conjugated secondary antibodies. The immunoreactive bands were visualized using an enhanced chemiluminescence solution (Thermo Scientific).

For ubiquitination assays, EC cells transfected with FLAG-p53, HA-ubiquitin with or without TSPYL5 or myc-USP7 were treated with 10 mM of MG132 (Sigma) for 8 h and then lysed in the FLAG lysis buffer (50 mM Tris–HCl, pH 8.0, 140 mM NaCl, 1 mM EDTA, 1% Triton X-100, 1% protease inhibitor cocktail I (GenDEPOT, Barker, TX, USA) and 1% protease inhibitor cocktail II (GenDEPOT). Cell lysates were incubated with 30 ml of anti-FLAG M2 affinity gel (Sigma) at 4 °C overnight. The bound FLAG-p53 was eluted with 20 μλ of FLAG peptide. The p53 ubiquitination was determined by western blotting using the haemagglutinin (HA) antibody (Santacruz).

Apoptosis assay

Apoptosis was examined by using an Annexin V-FITC/PI apoptosis detection kit (BD Pharmacy, Franklin Lakes, NJ, USA). HUVECs were treated with 0.1 mM H_2O_2 for 16 h to induce apoptosis. After washing with PBS, the cells were collected and resuspended with 500 μl of 1× binding buffer, to which Annexin V-FITC and PI solution was treated for 15 min at room temperature in the dark. Apoptosis was analyzed using flow cytometer BD Accuri C6 (BD Biosciences).

Animals

Male 8-week-old Balb/c-Nude mice were obtained from Dae han BioLink (Chungbuk, Korea) and maintained at the Korea Research Institute of Bioscience and Biotechnology (KRIBB). All mice were maintained under specific pathogen-free conditions and housed at a standard temperature (20–22 °C) and humidity (50–60%) in a controlled environment with a 12 h light/dark cycle and free access to food and water. All animal experiments were approved by the Institutional Animal Care and Use Committee of KRIBB.

Matrigel plug assay

Seven-week-old male nude mice (BalB/cAnNCriBgi-nu; Orient Bio, Korea) received a subcutaneous injection of 0.6 ml of Matrigel containing 1×10^6 HUVECs, 1×10^6 HUVECs plus 500 ng/ml VEGF, or TSPYL5-overexpressing HUVECs. The injected Matrigel rapidly formed a single, solid plug. After 11 days, the Matrigel plugs were surgically excised from the mice without connective tissues.

Wound healing studies

To evaluate the effect of TSPYL5 on wound healing, an excisional full-thickness wound model was used in this study. The mice were divided into five groups as follows: in group I, wounds were treated with only the DPBS control; in group II, wounds were treated with shTSPYL5; in group III, wounds were treated with ECs only; in group IV, wounds were treated with TSPYL5; and in group V, wounds were treated with TSPYL5 plus VEGF. All treatments were administered every other day.

Mice in all groups were anesthetized with an intraperitoneal injection of 2.5% 2,2,2-Tribromoethanol (Avertin, Sigma-Aldrich, St. Louis, MO, USA). Excisional wounds were made with a 6-mm biopsy punch (Integra Miltex, Davies Dr, York, PA, USA) on the backs of the mice. The cells were diluted in DPBS (5×10^4 cells/μl), and 20 μl of cell suspension containing 1×10^6 cells was applied at the wound site. To evaluate the effect of TSPYL5 on skin wound healing, the wound size of each mouse was measured on days 0, 3, 7 and 14 after surgery. Wound closure was calculated using the following formula: Wound closure (%) = [(Wound area of day 0—Wound area of day n)/Wound area of day 0] × 100.

To evaluate skin remodeling, histological and immunohistochemical analysis of the wounds was performed on mice that were sacrificed on 14 days after wounding. For the histological analysis, wound skin tissue samples were fixed overnight in 10% neutral buffered formalin followed by paraffin embedding. Then, embedded samples were cut into 10-μm-thick sections. The sections were subjected to H&E staining and Masson trichrome (Polysciences, Cat no. 25088-1) staining. For immunohistochemistry, the sections were deparaffinized in sodium citrate for 15 min at 121 °C to retrieve epitope structure and rehydrated with ethanol. And the sections were permeabilized with 0.1% Triton X-100 followed by blocking with 10% BSA at 37 °C for 1 h. After that, the sectioned tissue samples were incubated with the primary antibody against keratin 14 (Thermo Fisher Scientific) or CD31 (Santacruz) at 4 °C overnight and the incubated with fluorescence-labeled secondary antibody for 1 h at room temperature. And then washed with PBS, and mounting including DAPI.

Statistical analysis

The data are presented as the mean ± standard deviation (SD) of at least three separate experiments. Comparisons

between two groups were analyzed using Student's *t*-test. $p < 0.05$ or $p < 0.01$ was considered to indicate statistical significance.

Results

TSPYL5 is enriched in human ECs

To investigate the relationship between the expression of TSPYL family members and endothelial cell function and angiogenesis, we first examined and compared the expression levels of the *TSPYL1-6* genes in undifferentiated human pluripotent stem cells (hPSCs), hPSC-differentiated embryonic bodies (EBs), hPSC-differentiated endothelial cells (hPSC–ECs), and primary human umbilical vein endothelial cells (HUVECs). Undifferentiated hPSCs, including H9 human embryonic stem cells (hESCs) and human induced pluripotent stem cells (hiPSCs) derived from four reprogramming factors (*OCT4, SOX2, KLF4*, and *cMYC*) showed very low or no detectable levels of *TSPYL* gene expression (Fig. 1a and Supplementary Fig. 1). Upon hPSC differentiation into EBs containing multiple cell lineages, the expression of *TSPYL* family member genes, including *TSPYL1, 2, 4*, and *5* (Fig. 1a and Supplementary Fig. 1), was upregulated, resulting in a greater diversity of TSPYL family members. Most noticeably, among the six members, the *TSPYL5* gene (Fig. 1a and Supplementary Fig. 1) and protein (Fig. 1b) were highly expressed in both hPSC-ECs and primary ECs. These findings suggest that distinct expression levels of respective TSPYL family members are associated with specific cell lineages, and moreover, high TSPYL5 expression is characteristic of the endothelial cell lineage and potentially related to EC function.

TSPYL5 positively influences human EC functions in vitro

To determine whether TSPYL5 expression plays a functional role in ECs, we investigated the impact of both ectopic expression and suppression of TSPYL5 on EC proliferation, apoptosis, migration, and tube formation. *pMX* retroviruses encoding *TSPYL5* and lentiviral *shRNA* vectors targeting *TSPYL5* were transduced into HUVECs and hESC-ECs for TSPYL5 overexpression and knockdown, respectively (Fig. 2a, b and Supplementary Fig. 3). We found that TSPYL5-overexpressing ECs showed a higher proliferation rate than untransduced control cells (Fig. 2a, b). Conversely, the proliferation rate of TSPYL5-knockdown ECs was markedly decreased (Fig. 2a, b). In addition, TSPYL5 overexpression significantly protected hydrogen peroxide (H_2O_2)-induced apoptosis, whereas TSPYL5 depletion enhanced apoptosis (Fig. 2c, d). Accordingly, the expression of pro-apoptotic Bax protein was markedly reduced by TSPYL5 overexpression and increased by TSPYL5 depletion (Fig. 3a). These results suggest that TSPYL5 acts as a pro-proliferative and anti-apoptotic factor in human ECs.

We further determined the effect of TSPYL5 expression on EC functions such as migration and tube formation. The transwell migration assay showed that

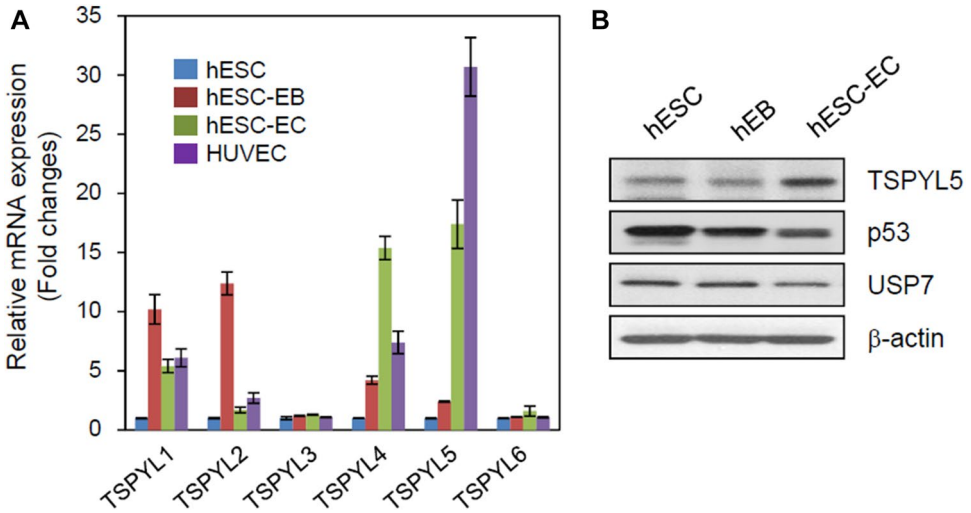

Fig. 1 Expression pattern of TSPYL family members in human ECs. **a** qPCR analysis of *TSPYL1-6* genes in H9 hESC, 7-day-old hESC-EB, hESC-EC, and HUVEC. The results are from four independent experiments. For all bar graphs, data are presented as the mean ± SD (n = 4). The *GAPDH* gene was used as a reference gene. **b** Western blot analysis of TSPYL5, p53, and USP7 proteins in H9 hESC, 7-day-old hEB, and hESC-EC. β–Actin was used as a loading control. Abbreviations: hESC, H9 human embryonic stem cell; hEB, hESC-derived EB; hESC-EC, hESC-differentiated endothelial cells; HUVEC, human umbilical vein endothelial cells; GAPDH, glyceraldehyde-3-phosphate dehydrogenase

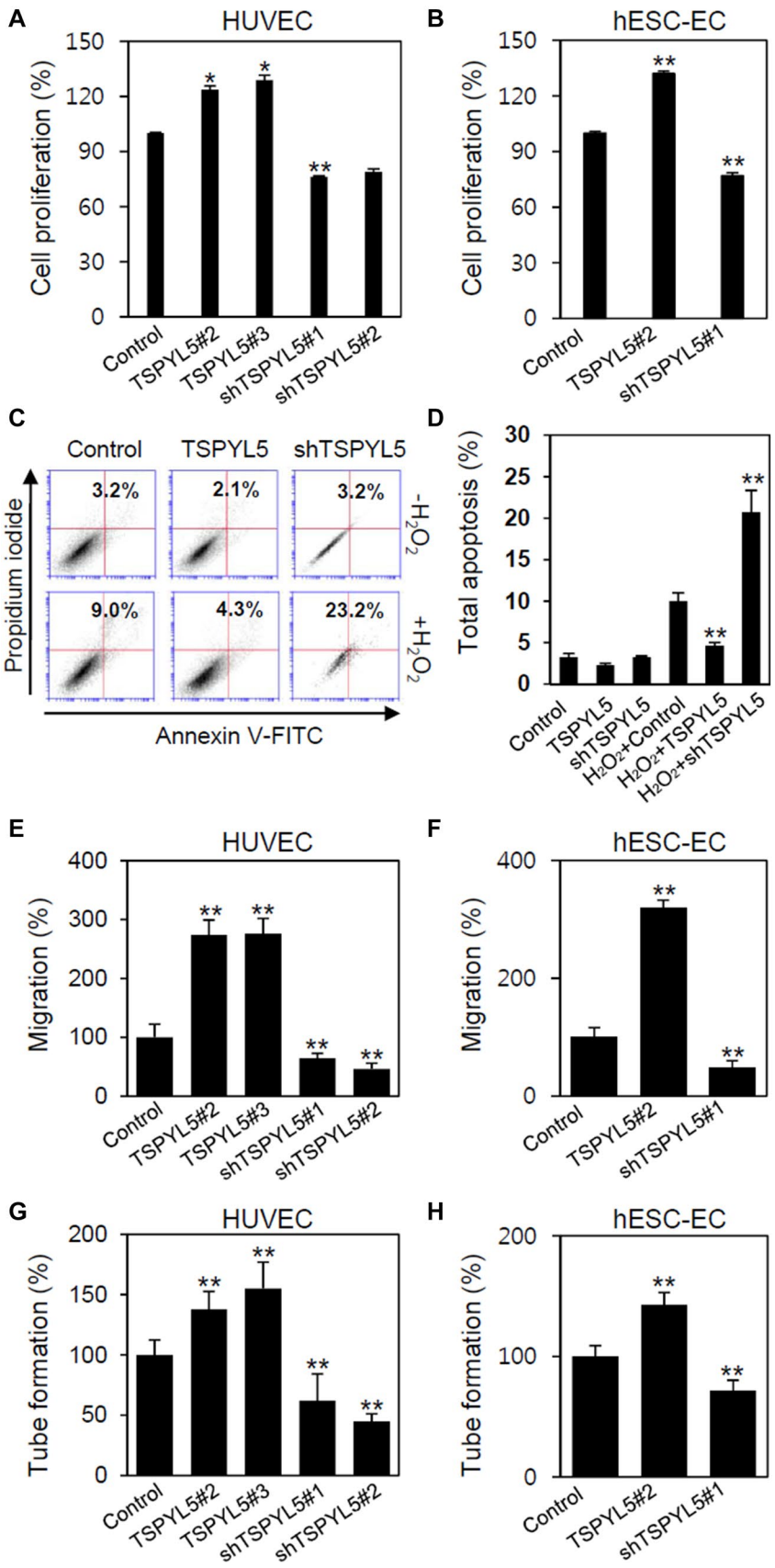

Fig. 2 TSPYL5 positively influences EC proliferation, migration, and tube formation in vitro. **a** Cell proliferation analysis of HUVEC after TSPYL5 overexpression or knockdown. 4 days after transduction of cells with the *pMX-TSPYL5* expression vector (TSPYL5) or *Lenti-shTSPYL5* (shTSPYL5), relative cell proliferation was determined by using the cell counting kit-8 (CCK-8). **b** Cell proliferation analysis of hESC-EC after *TSPYL5* overexpression or knockdown. 4 days after transduction of cells with TSPYL5 or shTSPYL5, relative cell proliferation was determined. **c** Cell apoptosis was analyzed in *TSPYL5*-overexpressed or *TSPYL5*-depleted HUVEC by flow cytometry, in which HUVEC was treated with 0.1 mM H_2O_2 for 16 h. **d** TSPYL5-overexpressing cells were significantly decrease in H_2O_2-induced apoptosis. **e, f** Cell migration of HUVEC or hESC-EC after *TSPYL5* overexpression or knockdown. 4 days after transduction with TSPYL5 or shTSPYL5, the migrated cells were stained with H&E. **g, h** Tube formation ability of HUVEC or hESC–EC after *TSPYL5* overexpression or knockdown. Data from two (HUVEC) or one (hESC–EC) representative infections and cell proliferation, migration, and tube formation assays for each condition are shown. All data are presented as the mean ± SD (n=3). $^{*}p<0.05$, $^{**}p<0.01$ versus untransduced cells. Control: untransduced cells

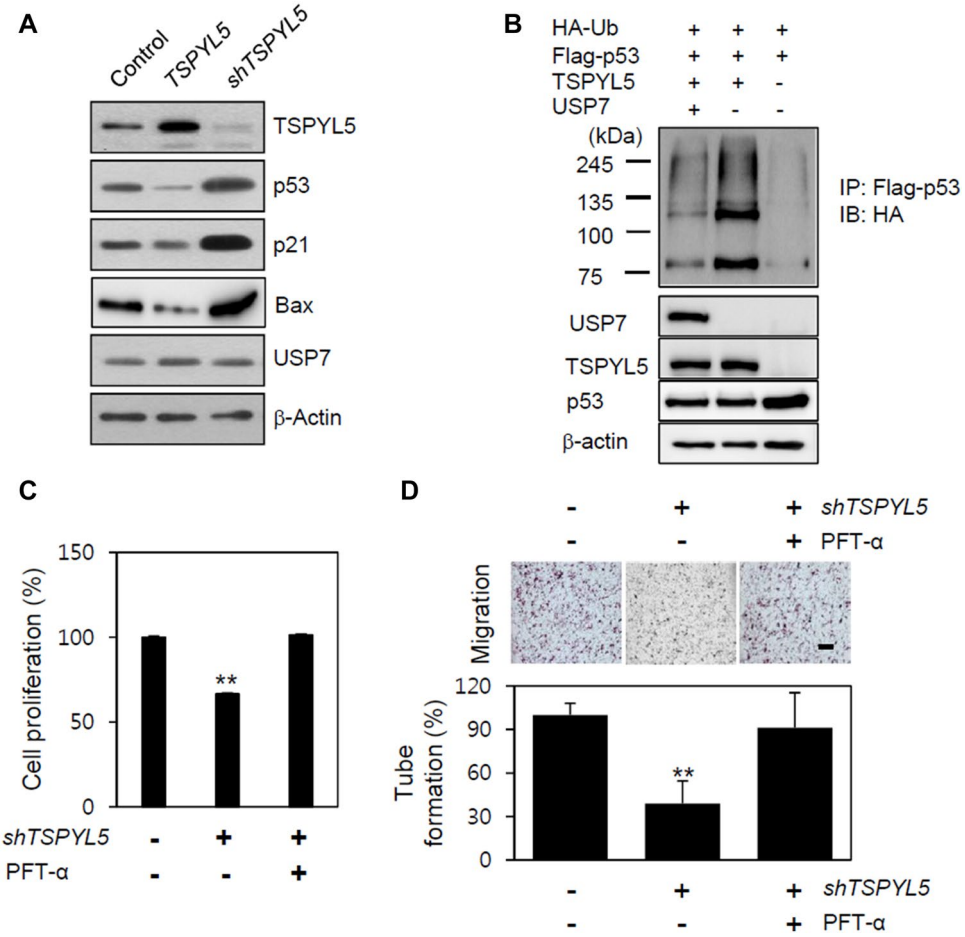

Fig. 3 TSPYL5-mediated functional regulations of ECs are associated with p53 signaling. **a** Western blot analysis of TSPYL5, p53, p21, Bax, and USP7 proteins in *TSPYL5*-overexpressed or *TSPYL5*-depleted HUVEC. HUVEC were harvested 4 days postinfection with the *pMX-TSPYL5* overexpression vector (TSPYL5) or *TSPYL5 Lenti-shRNA* (shTSPYL5). β−Actin was used as a loading control. **b** Ubiquitination of p53 was examined in HUVEC. Overexpression of TSPYL5 induced an increase in p53 ubiquitination compared with overexpression of FLAG-p53 and HA-ubiquitin without TSPYL5, in which the overexpression of USP-7 promoted deubiquination of p53. Ubiquination of p53 was determined by using HA antibody. **c** Cell proliferation analysis after TSPYL5 depletion in the presence or absence of p53 inhibition in HUVECs. HUVECs were infected with TSPYL5 Lenti-shRNA (shTSPYL5) in the presence or absence of the p53 inhibitor PFT-α (25 μM), and after 4 days, relative cell proliferation was determined by using CCK-8. Data are presented as the mean ± SD (n=3). $^{**}p < 0.01$ versus uninfected cells. **d** Migration and tube formation ability of HUVECs after TSPYL5 depletion in the presence or absence of p53 inhibition. HUVECs were infected with TSPYL5 Lenti-shRNAs (shTSPYL5) in the presence or absence of PFT-α (25 μM), and 4 days post-transduction, the migrated cells were stained with hematoxylin and eosin. Representative images depicting the formation of capillary-like tube structures by HUVECs on Matrigel were taken 4 days postinfection with shTSPYL5 in the presence or absence of PFT-α (25 μM). Data are presented as the mean ± SD (n= 3). $^{**}p < 0.01$ versus uninfected cells. Scale bar: 50 μm. Control: untransduced cells

TSPYL5-overexpressing HUVECs and hESC-ECs exhibited a markedly increased migratory capacity compared with the untransduced control cells (Fig. 2e, f and Supplementary Fig. 2). In contrast, TSPYL5-depleted ECs exhibited a decreased migratory capacity compared with the control cells (Fig. 2e, f). Furthermore, TSPYL5 overexpression led to more extensive tube networks forming elongated and robust tube-like structures and more cell connections on Matrigel than observed in untransduced controls or TSPYL5-depleted ECs (Fig. 2g, h). These results indicate that TSPYL5 can potentiate EC functions in vitro.

TSPYL5 influences on human EC functions through p53 inhibition

Ubiquitin-specific protease 7 (USP7), the major p53 deubiquitylase, interacts with p53 and is responsible for p53 stabilization [23]. TSPYL5 has been implicated as a negative regulator of p53 function through its interaction with USP7 [24]. On the basis of such studies, we investigated the possibility that p53 is a downstream target of TSPYL5 in human ECs. To clarify the molecular mechanism underlying the TSPYL5-induced promotion of EC functions, we

investigated whether TSPYL5 expression influences p53 expression. Overexpression of TSPYL5 in HUVECs significantly decreased the protein expression of p53 and its downstream target p21 compared to expression of the control (Fig. 3a). Conversely, TSPYL5 depletion in HUVECs increased the protein expression of p53 and p21 compared to the control (Fig. 3a). The expression levels of USP7 were not noticeably affected by changes in TSPYL5 expression in HUVECs (Fig. 3a). We further tested whether TSPYL5-mediated down-regulation of p53 protein levels is associated with p53 ubiquitination status. Ubiquitination assays confirmed that TSPYL5 overexpression resulted in an increase of ubiquitinated p53 (Fig. 3b). However, co-expression of USP7 with TSPYL5 appeared to block p53 ubiquitination (Fig. 3b). These results indicate that TSPYL5-mediated effects in hECs are closely associated with p53 levels negatively regulated by USP7-mediated p53 ubiquitination.

To further clarify the molecular association between TSPYL5 and p53 in the context of EC functions, we examined whether the TSPYL5 depletion-mediated loss of EC functions could be restored by p53 inhibition. We found that the reductions in EC proliferation (Fig. 3c), migration, and tube formation (Fig. 3d) mediated by TSPYL5 depletion were considerably restored by pre-treatment with 10 μg/ml pifithrin-α (PFT-α), a specific inhibitor of p53, for 24 h. These results strongly suggest that p53 is a downstream target of TSPYL5 in human ECs.

Exposure to adriamycin (50 nM) for 3 days caused premature senescence in HUVECs, as evidenced by the positive expression of senescence-associated β−galactosidase (Fig. 4a) and the immunofluorescence detection of increased microtubule disruption using anti-β-tubulin (Fig. 4b). Significantly, TSPYL5-overexpressing HUVECs were largely resistant to adriamycin-induced senescence (Fig. 4a, b). We also found that adriamycin-treated HUVECs showed increased expression of senescence-associated p53 and p21 proteins, and this increase was significantly blocked by TSPYL5 overexpression (Fig. 4c). TSPYL5 expression also prevented the senescence-associated down-regulation of Sirt1 in adriamycin-treated HUVECs; rather, Sirt1 expression was upregulated (Fig. 4c). These findings suggest that the TSPYL5-induced promotion of EC functions may also be associated with the protective role of Sirt1 against p53-mediated senescence.

TSPYL5-overexpressing ECs show potently enhanced angiogenesis in vivo

To further verify the pro-angiogenic effect of TSPYL5, Matrigel plug and wound healing assays were performed using TSPYL5-overexpressing or TSPYL5-depleted stable HUVECs in vivo. For the Matrigel plug assay, Matrigel containing HUVECs (Control), recombinant VEGF (500 ng/ml), or TSPYL5-overexpressing HUVECs (TSPYL5) were injected into the flanks of BALB/c mice. After 1 week, the mice were sacrificed, and the Matrigel plugs were removed. Matrigel plugs containing VEGF or TSPYL5-overexpressing HUVECs exhibited a red color, indicating the occurrence of angiogenesis (Fig. 5). In contrast, Matrigel plugs containing only HUVECs were light red or pale yellow (Fig. 5). These

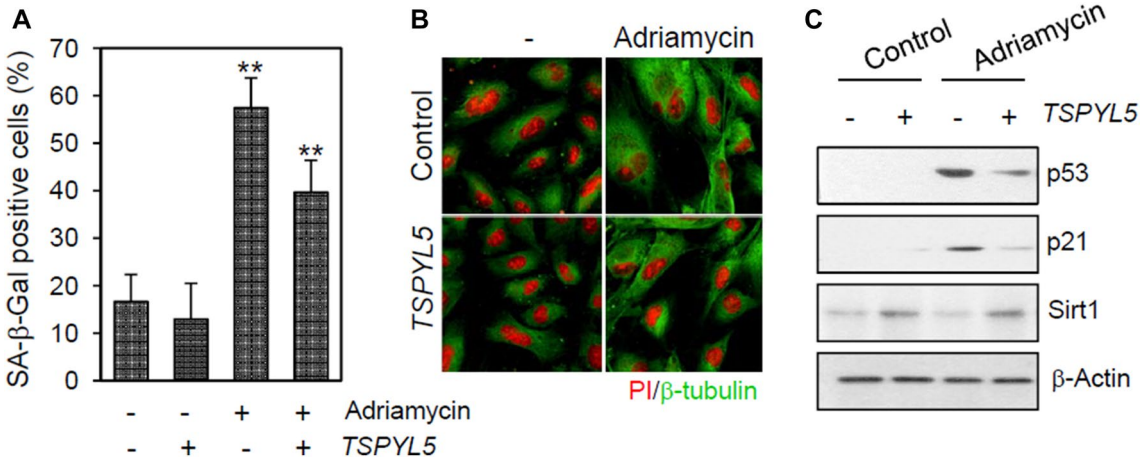

Fig. 4 TSPYL5 inhibits adriamycin-induced senescence in human ECs. **a** SA-β-gal staining of HUVEC infected with control viral particles (−) or *pMX-TSPYL5* (+) in the absence (−) or presence (+) of 1 μM adriamycin. 4 days postinfection, SA-β-gal-positive cells were detected with a cellular senescence assay kit and counted in 4 independent fields under a microscope. Data are presented as the mean ± SD ($n=3$). $^{**}p < 0.01$ versus uninfected cells. **b** Immunocytochemical analysis of β-tubulin in HUVEC infected with control viral particles (−) or pMX-TSPYL5 (+) in the absence (−) or presence (+) of 1 μM adriamycin. PI was used as a nuclear counterstain for immunofluorescence analysis. Scale bars: 50 μm. **c** Western blot analysis of p53, p21, and Sirt1 proteins in HUVEC with (+) or without TSPYL5 overexpression (−) in the absence (−) or presence (+) of 1 μM adriamycin. Abbreviations: SA-β-gal, Senescence-associated β-galactosidase; PI, Propidium iodide

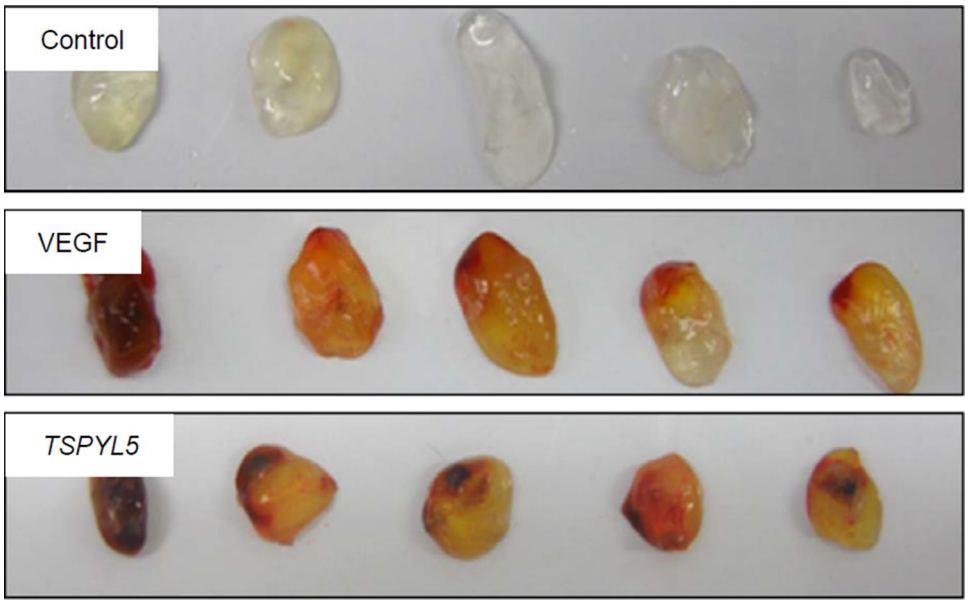

Fig. 5 Representative Matrigel plugs containing control (HUVEC only), VEGF (500 ng/ml), or TSPYL5-overexpressing HUVEC. Plugs were removed from mice at day 11. A red color indicates abundant red blood cells. Five mice were used in each group

findings indicate that TSPYL5-overexpressing HUVECs exhibited enhanced angiogenic properties with a potency comparable to pro-angiogenic VEGF treatment in vivo.

To examine the effects of TSPYL5 on skin wound healing, a wound healing mouse model was used. Full-thickness sections of skin were removed from the backs of mice using a 6-mm biopsy punch at various positions. On the same day, mice were treated with either control DPBS, recombinant VEGF, HUVECs, or TSPYL5-overexpressing or TSPYL5-depleted stable HUVECs, and the wound size was measured on days 0, 3, 7, and 14 to monitor the regeneration process. Skin wounds treated with TSPYL5-overexpressing HUVECs healed significantly faster than those in the other groups and showed complete healing at approximately 12 days after injury (Fig. 6a, b). On day 7, the wound size relative to day 0 was significantly reduced, and the differences in wound closure among groups were significant, as follows: on day 7, the wound closure was 23.71 ± 9.07% for the DPBS-treated group, 31.56 ± 10.26% for the HUVEC-treated group, 14.21 ± 1.25% for the TSPYL5-depleted HUVEC-treated group, 47.40 ± 4.05% for the VEGF-treated group, and 57.69 ± 2.38% for the TSPYL5-overexpressing HUVEC-treated group. On day 14, the DPBS-, HUVEC-, and TSPYL5-depleted stable HUVEC-treated groups showed incomplete wound healing (Fig. 6a, b).

For histological analysis of the re-epithelialization of the wound area, wound tissues collected from each group on day 14 were sectioned and stained with H&E and Masson's trichrome stain. Notably, the TSPYL5-overexpressing HUVEC-treated group showed enhanced re-epithelialization relative to the other groups, and the newly formed epidermal layer displayed great similarity to the surrounding epidermis (Fig. 6c). In addition, the TSPYL5-overexpressing HUVEC-treated group showed organized collagen deposition, and the degree of collagen deposition within the wound site was not significantly different compared to that in the other groups (Fig. 6c). The TSPYL5-overexpressing HUVEC-treated group also showed the same expression pattern of epithelial cell marker cytokeratin 14, expressed late in wound healing, in the regenerated wound site as that observed in naïve epithelium, while shTSPYL5-HUVEC injected groups showed impaired cytokeratin 14 expression (Fig. 6c). Importantly, TSPYL5-mediated enhancement of wound healing was found to be associated with CD31-positive site within wound area (Fig. 6d). These results suggest that TSPYL5 overexpression improved wound healing through enhancing angiogenesis in vivo.

Discussion

The expression and function of TSPYLs has been primarily examined in highly proliferating human cancer cells and immortalized cells but is largely undefined in normal, terminally differentiated cell types with specialized functions, such as endothelial cells. Our observations show that changes in the expression levels of TSPYL family members were dependent on the cell type composition of the population. TSPYLs were expressed in undifferentiated hPSCs (ESCs and iPSCs) at low levels compared to differentiated cells, and their expression pattern was altered with inter-individual variability following differentiation (Fig. 1 and Supplementary Fig. 1). While TSPYL3 and 6 expression was not noticeably changed, TSPYL1, 2, 4, and 5 expression was variably increased in spontaneously differentiating EBs, which potentially contain multiple somatic cell types,

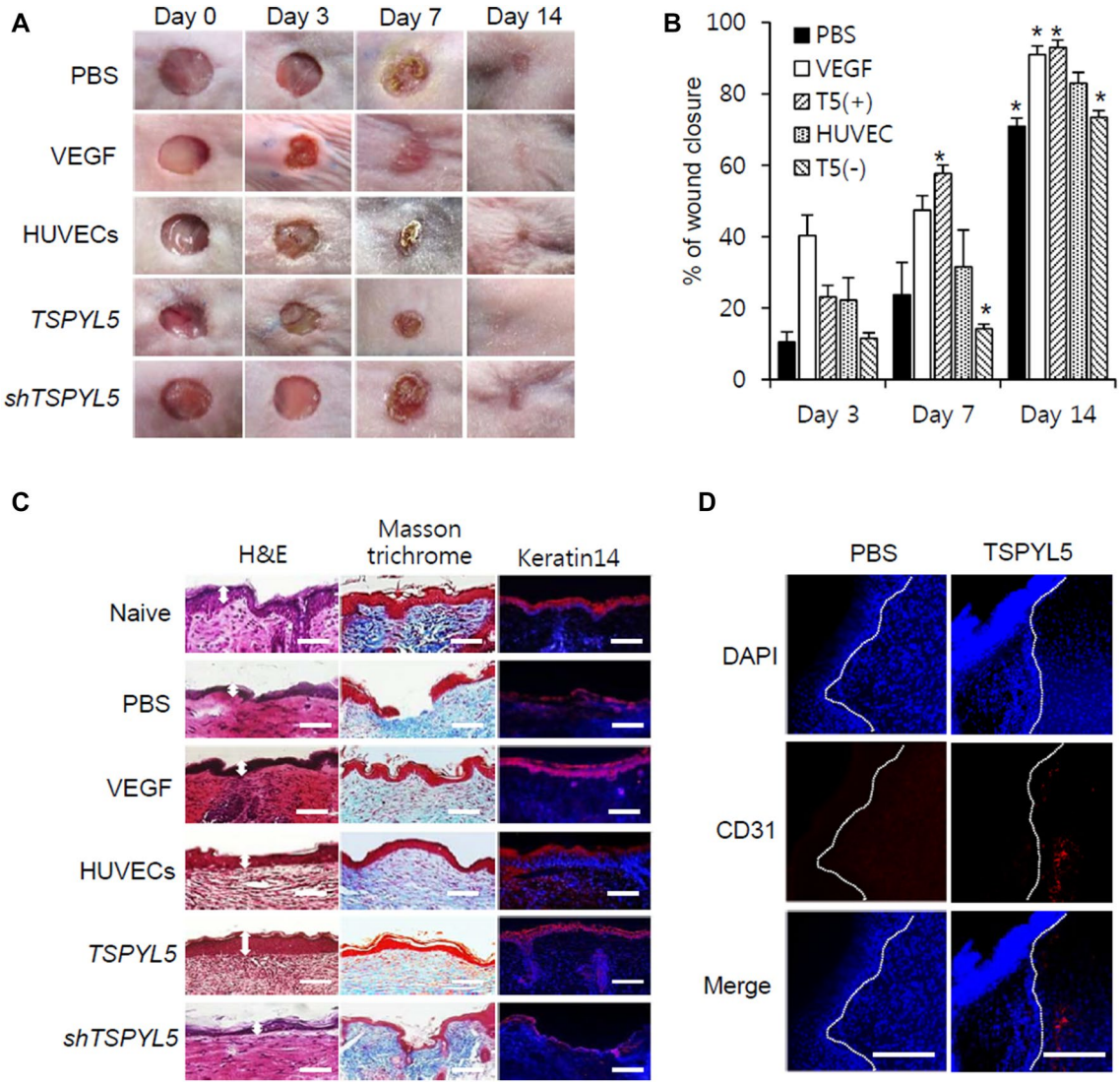

Fig. 6 TSPYL5 overexpression improves the quality of skin wound healing. Mouse skin wounds generated by 6-mm punch biopsy were treated with either control PBS, VEGF (500 ng/ml), HUVEC, or TSPYL5-overexpressing or TSPYL5-depleted stable HUVEC. **a** Representative images of wound healing in mice with the indicated treatments at day 0, 3, 7 and 14 after cutaneous punch biopsy. **b** Comparison of the % of the open wound size at days 7 and 14 between HUVEC control and TSPYL5-overexpressing or TSPYL5-depleted HUVEC-treated mice. TSPYL5-overexpressing HUVEC significantly improved the rate of wound closure in mice compared with that of HUVEC control-treated mice. $^{*}p < 0.05$ versus untransduced HUVEC. Data are presented as the mean ± SD (n = 6). **c** Representative images of H&E, Masson's Trichrome staining, and immunofluorescent staining of keratin 14 in unwounded (naïve) or wounded skin sites with the indicated treatments on days 14 after wounding. Scale bars: 500 µm. **d** Immunohistochemical analysis of CD31 in wounded skin sites with treatments of PBS or TSPYL5-overexpressing cells on day 7 after wounding. DAPI was used as a nuclear counterstain for immunofluorescence analysis. Dotted lines indicate the dermo-epidermal junction. Scale bars: 500 µm

compared to undifferentiated hPSCs (Fig. 1 and Supplementary Fig. 1).

Among the TSPYL genes, TSPYL5 (also known as KIAA1750, located on chromosome 8q22) was prominently enriched in the normal human ECs investigated (hESCs, hiPSC-differentiated ECs and primary HUVECs) (Fig. 1 and Supplementary Fig. 1). Although the role of TSPYL5 in hPSCs is unclear, high-passage hPSCs display hypermethylation-mediated down-regulation of TSPYL5 that appears to be favorable for the maintenance of pluripotency by mediating the down-regulation of differentiation-related genes and the upregulation of pluripotency-related genes [25]. Another member of the NAP family, NAP1-like 1 (Nap1l1), was also found to positively regulate murine PSC proliferation by activating ERK or AKT signaling and downregulating p21 and p27. Our findings suggest that the upregulation of TSPYL5 may be beneficial for inducing the loss of pluripotency and inducing differentiation, specifically

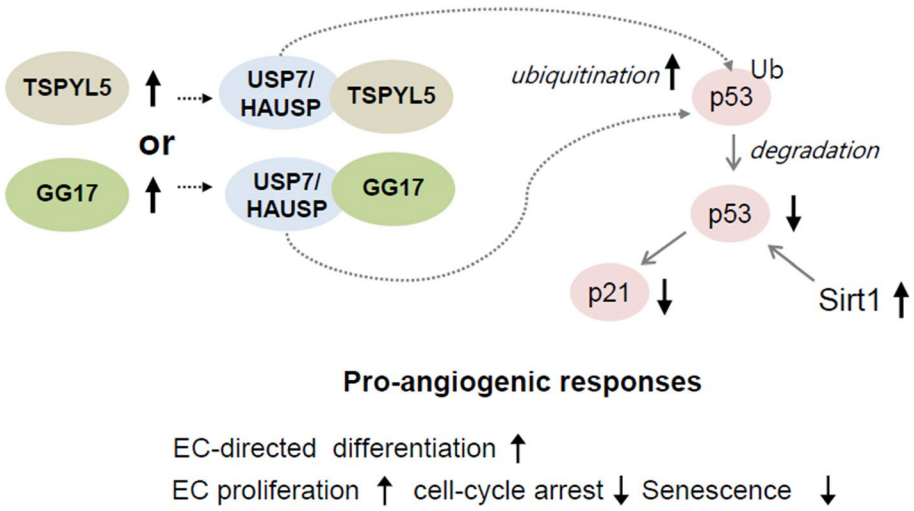

Fig. 7 Graphical summary of TSPYL5-mediated pro-angiogenic regulation of EC functions

into the endothelial lineage. Our findings further suggest that TSPYL5 is associated with endothelial functions.

High expression of NAP1 has been reported to be positively associated with the rapid proliferation and blood vessel formation of pulmonary microvascular endothelial cells (PMVECs) but to have no influence on EC phenotype specification [26]. Consistent with a role for NAP1 in EC functions, our findings demonstrate that TSPYL5 expression is required for the maintenance of EC functions. TSPYL5 depletion resulted in decreased proliferation, migration, and tube formation in both HUVECs and hPSC-ECs (Fig. 2). Notably, TSPYL5 expression was increased upon hPSC differentiation into ECs (Fig. 1 and Supplementary Fig. 1), suggesting that unlike NAP1, TSPYL5 appears to contribute to EC lineage specification. TSPYL5 overexpression appeared to potentially enhance proliferation, migration and tube formation (Fig. 2) and block senescence in cultured ECs in vitro (Fig. 4). Our results also provide evidence for pro-angiogenic effects of TSPYL5 in vivo, confirmed by the enhanced vessel formation in Matrigel plugs (Fig. 5), as well as by the improved healing of cutaneous wounds, possibly due to improved EC function, in an in vivo mouse wound healing model (Fig. 6). These findings suggest that TSPYL5 has significant impacts on various EC functions and angiogenesis and that TSPYL members have varied and distinct roles in different cell types.

TSPYL5 has been shown to mediate the acceleration of cell proliferation in several cell types, including A549 lung adenocarcinoma cells, HepG2 hepatoblastoma cells, human normal immortalized cells (HEK293 embryonic kidney cells), and spermatogonia [27, 28]. The DNA methylation-mediated silencing of TSPYL5 contributes to its tumor-suppressor properties in glioma [8]. Although the underlying mechanism of TSPYL5 remains ambiguous, molecular targets and mechanisms of action involved in TSPYL5-mediated proliferation have been proposed. Notably, TSPYL5 acts as a negative regulator of p53-mediated growth arrest in various cell types, including breast cancer [24]. An interaction between TSPYL5 and ubiquitin-specific protease 7 (USP7; also known as herpesvirus-associated ubiquitin-specific protease; HAUSP) results in an impaired interaction between p53 and USP7, leading to increased p53 ubiquitination and degradation in breast cancer [24]. MUC16 (in a family of high-molecular weight O-glycosylated proteins known as mucins) was identified as an important regulator of the TSPYL5-mediated down-regulation of p53 via promotion of the JAK2/STAT3/GR signaling axis for lung cancer cell growth and metastasis [29]. One of the interacting partners of TSPYL5, TSPY1, acts as a suppressor of USP7-mediated p53 degradation in promoting spermatogonial proliferation in a TSPYL5-dependent and TSPYL5-independent manner [28].

The accumulation of p53 in ECs has been reported to be associated with cell cycle arrest, senescence, apoptotic cell death, and impaired angiogenesis and cardiac functions [30–32]. Consistently, our results provide evidence that the TSPYL5-mediated promotion of EC proliferation and function is associated with p53 (Fig. 7). TSPYL5 overexpression resulted in a marked decrease of p53 and its downstream target p21 (Fig. 3). The suppression of p53 function by the p53 inhibitor pifithrin-α blocked the TSPYL5-depletion-mediated down-regulation of EC proliferation, migration and tube formation (Fig. 3). Importantly, TSPYL5 overexpression was highly effective at protecting HUVECs from adriamycin-induced senescence through influencing the p53/p21/Sirt1 signaling axis (Fig. 3). These observations confirmed that precise modulation of p53 activity is important and required for maintaining EC function and angiogenesis and suggested that the TSPYL5-mediated p53 pathway is an important molecular mechanism underlying EC-mediated events (Fig. 7).

In conclusion, we demonstrate a novel role for TSPYL5 in regulating EC functions and angiogenesis, and we emphasize that the physiological features and roles of TSPYLs occur in a tissue- or cell type-specific manner. Further cellular and molecular studies of the function of TSPYL5 in ECs may lead to a clear and fundamental understanding of the molecular mechanisms that modulate angiogenesis and may reveal more robust target genes and functions of TSPYL5-mediated physiologic and pathologic responses involved in neovascularization.

Acknowledgements This work was supported by National Research Foundation of Korea (NRF) (Grant No. 2017R1A2B2012190) and NST (Grant No. CRC-15-02-KRIBB) grants from the Korean government (MSIP).

Author contributions H-JN: Conception and design, data analysis and interpretation, manuscript writing, final approval of manuscript. CEY: Conception and design, data analysis and interpretation, manuscript writing, final approval of manuscript. H-SK: Collection and assembly of data, data analysis and interpretation, manuscript writing, final approval of manuscript. JL: Conception and design, data analysis and interpretation. J-YK: Collection and assembly of data, manuscript writing. YSC: Conception and design, data analysis and interpretation, financial support, manuscript writing, final approval of manuscript.

Compliance with ethical standards

Conflict of interest The authors have declared no potential conflicts of interest.

References

1. Arnemann J, Jakubiczka S, Thuring S, Schmidtke J (1991) Cloning and sequence analysis of a human Y-chromosome-derived, testicular cDNA, TSPY. Genomics 11(1):108–114
2. Schnieders F, Dork T, Arnemann J, Vogel T, Werner M, Schmidtke J (1996) Testis-specific protein, Y-encoded (TSPY) expression in testicular tissues. Hum Mol Genet 5(11):1801–1807
3. Lau Y, Chou P, Iezzoni J, Alonzo J, Komuves L (2000) Expression of a candidate gene for the gonadoblastoma locus in gonadoblastoma and testicular seminoma. Cytogenet Cell Genet 91(1–4):160–164. https://doi.org/10.1159/000056838
4. Su MT, Lee IW, Kuo PL (2006) Presence of TSPY transcript and absence of transcripts of other Y chromosomal genes in a case of microscopic gonadoblastoma. Gynecol Oncol 103(1):357–360. https://doi.org/10.1016/j.ygyno.2006.05.010
5. Dasari VK, Goharderakhshan RZ, Perinchery G, Li LC, Tanaka Y, Alonzo J, Dahiya R (2001) Expression analysis of Y chromosome genes in human prostate cancer. J Urol 165(4):1335–1341
6. Vogel T, Dittrich O, Mehraein Y, Dechend F, Schnieders F, Schmidtke J (1998) Murine and human TSPYL genes: novel members of the TSPY-SET-NAP1L1 family. Cytogenet Cell Genet 81(3–4):265–270. https://doi.org/10.1159/000015042
7. Dechend F, Williams G, Skawran B, Schubert S, Krawczak M, Tyler-Smith C, Schmidtke J (2000) TSPY variants in six loci on the human Y chromosome. Cytogenet Cell Genet 91(1–4):67–71. https://doi.org/10.1159/000056821
8. Kim TY, Zhong S, Fields CR, Kim JH, Robertson KD (2006) Epigenomic profiling reveals novel and frequent targets of aberrant DNA methylation-mediated silencing in malignant glioma. Cancer Res 66(15):7490–7501. https://doi.org/10.1158/0008-5472.CAN-05-4552
9. Lin CW, Huang TN, Wang GS, Kuo TY, Yen TY, Hsueh YP (2006) Neural activity- and development-dependent expression and distribution of CASK interacting nucleosome assembly protein in mouse brain. J Comp Neurol 494(4):606–619. https://doi.org/10.1002/cne.20825
10. Tao KP, Fong SW, Lu Z, Ching YP, Chan KW, Chan SY (2011) TSPYL2 is important for G1 checkpoint maintenance upon DNA damage. PLoS ONE 6(6):e21602. https://doi.org/10.1371/journal.pone.0021602
11. Wang GS, Hong CJ, Yen TY, Huang HY, Ou Y, Huang TN, Jung WG, Kuo TY, Sheng M, Wang TF, Hsueh YP (2004) Transcriptional modification by a CASK-interacting nucleosome assembly protein. Neuron 42(1):113–128
12. Hsueh YP (2006) The role of the MAGUK protein CASK in neural development and synaptic function. Curr Med Chem 13(16):1915–1927
13. Epping MT, Lunardi A, Nachmani D, Castillo-Martin M, Thin TH, Cordon-Cardo C, Pandolfi PP (2015) TSPYL2 is an essential component of the REST/NRSF transcriptional complex for TGFbeta signaling activation. Cell Death Differ 22(8):1353–1362. https://doi.org/10.1038/cdd.2014.226
14. Roth LM, Cheng L (2015) Expression of Transcription Factors and Nuclear Receptors in Mixed Germ Cell-Sex Cord Stromal Tumor and Related Tumors of the Gonads. Int J Gynecol Pathol 34(6):528–534. https://doi.org/10.1097/PGP.0000000000000192
15. Kido T, Lo RC, Li Y, Lee J, Tabatabai ZL, Ng IO, Lau YF (2014) The potential contributions of a Y-located protooncogene and its X homologue in sexual dimorphisms in hepatocellular carcinoma. Hum Pathol 45(9):1847–1858. https://doi.org/10.1016/j.humpath.2014.05.002
16. Puffenberger EG, Hu-Lince D, Parod JM, Craig DW, Dobrin SE, Conway AR, Donarum EA, Strauss KA, Dunckley T, Cardenas JF, Melmed KR, Wright CA, Liang W, Stafford P, Flynn CR, Morton DH, Stephan DA (2004) Mapping of sudden infant death with dysgenesis of the testes syndrome (SIDDT) by a SNP genome scan and identification of TSPYL loss of function. Proc Natl Acad Sci USA 101(32):11689–11694. https://doi.org/10.1073/pnas.0401194101
17. de Andrade TG, Peterson KR, Cunha AF, Moreira LS, Fattori A, Saad ST, Costa FF (2006) Identification of novel candidate genes for globin regulation in erythroid cells containing large deletions of the human beta-globin gene cluster. Blood Cells Mol Dis 37(2):82–90. https://doi.org/10.1016/j.bcmd.2006.07.003
18. Moey C, Hinze SJ, Brueton L, Morton J, McMullan DJ, Kamien B, Barnett CP, Brunetti-Pierri N, Nicholl J, Gecz J, Shoubridge C (2016) Xp11.2 microduplications including IQSEC2, TSPYL2 and KDM5C genes in patients with neurodevelopmental disorders. Eur J Hum Genet 24(3):373–380. https://doi.org/10.1038/ejhg.2015.123
19. Grasberger H, Bell GI (2005) Subcellular recruitment by TSG118 and TSPYL implicates a role for zinc finger protein 106 in a novel developmental pathway. Int J Biochem Cell Biol 37(7):1421–1437. https://doi.org/10.1016/j.biocel.2005.01.013
20. Liu M, Ingle JN, Fridley BL, Buzdar AU, Robson ME, Kubo M, Wang L, Batzler A, Jenkins GD, Pietrzak TL, Carlson EE, Goetz MP, Northfelt DW, Perez EA, Williard CV, Schaid DJ, Nakamura Y, Weinshilboum RM (2013) TSPYL5 SNPs: association with plasma estradiol concentrations and aromatase expression. Mol Endocrinol 27(4):657–670. https://doi.org/10.1210/me.2012-1397
21. Son MY, Choi H, Han YM, Cho YS (2013) Unveiling the critical role of REX1 in the regulation of human stem cell pluripotency. Stem cells 31(11):2374–2387. https://doi.org/10.1002/stem.1509

22. Yoo CH, Na HJ, Lee DS, Heo SC, An Y, Cha J, Choi C, Kim JH, Park JC, Cho YS (2013) Endothelial progenitor cells from human dental pulp-derived iPS cells as a therapeutic target for ischemic vascular diseases. Biomaterials 34(33):8149–8160. https://doi.org/10.1016/j.biomaterials.2013.07.001
23. Li M, Chen D, Shiloh A, Luo J, Nikolaev AY, Qin J, Gu W (2002) Deubiquitination of p53 by HAUSP is an important pathway for p53 stabilization. Nature 416(6881):648–653. https://doi.org/10.1038/nature737
24. Epping MT, Meijer LA, Krijgsman O, Bos JL, Pandolfi PP, Bernards R (2011) TSPYL5 suppresses p53 levels and function by physical interaction with USP7. Nat Cell Biol 13(1):102–108. https://doi.org/10.1038/ncb2142
25. Weissbein U, Plotnik O, Vershkov D, Benvenisty N (2017) Culture-induced recurrent epigenetic aberrations in human pluripotent stem cells. PLoS Genet 13(8):e1006979. https://doi.org/10.1371/journal.pgen.1006979
26. Clark J, Alvarez DF, Alexeyev M, King JA, Huang L, Yoder MC, Stevens T (2008) Regulatory role for nucleosome assembly protein-1 in the proliferative and vasculogenic phenotype of pulmonary endothelium. Am J Physiol Lung Cell Mol Physiol 294(3):L431–L439. https://doi.org/10.1152/ajplung.00316.2007
27. Kim EJ, Lee SY, Kim TR, Choi SI, Cho EW, Kim KC, Kim IG (2010) TSPYL5 is involved in cell growth and the resistance to radiation in A549 cells via the regulation of p21(WAF1/Cip1) and PTEN/AKT pathway. Biochem Biophys Res Commun 392(3):448–453. https://doi.org/10.1016/j.bbrc.2010.01.045
28. Shen Y, Tu W, Liu Y, Yang X, Dong Q, Yang B, Xu J, Yan Y, Pei X, Liu M, Xu W, Yang Y (2018) TSPY1 suppresses USP7-mediated p53 function and promotes spermatogonial proliferation. Cell Death Dis 9(5):542. https://doi.org/10.1038/s41419-018-0589-7
29. Lakshmanan I, Salfity S, Seshacharyulu P, Rachagani S, Thomas A, Das S, Majhi PD, Nimmakayala RK, Vengoji R, Lele SM, Ponnusamy MP, Batra SK, Ganti AK (2017) MUC16 regulates TSPYL5 for lung cancer cell growth and chemoresistance by suppressing p53. Clin Cancer Res 23(14):3906–3917. https://doi.org/10.1158/1078-0432.CCR-16-2530
30. Grillari J, Hohenwarter O, Grabherr RM, Katinger H (2000) Subtractive hybridization of mRNA from early passage and senescent endothelial cells. Exp Gerontol 35(2):187–197
31. Morimoto Y, Bando YK, Shigeta T, Monji A, Murohara T (2011) Atorvastatin prevents ischemic limb loss in type 2 diabetes: role of p53. J Atheroscler Thromb 18(3):200–208
32. Gogiraju R, Xu X, Bochenek ML, Steinbrecher JH, Lehnart SE, Wenzel P, Kessel M, Zeisberg EM, Dobbelstein M, Schafer K (2015) Endothelial p53 deletion improves angiogenesis and prevents cardiac fibrosis and heart failure induced by pressure overload in mice. J Am Heart Assoc 4 (2):e001770. https://doi.org/10.1161/JAHA.115.001770